PAPER • OPEN ACCESS

Analysis of an unmitigated 2-inch cold leg LOCA transient with ASTEC and MELCOR codes

To cite this article: G Agnello *et al* 2022 *J. Phys.: Conf. Ser.* **2177** 012024

View the article online for updates and enhancements.

You may also like

Analysis of an unmitigated 2-inch cold leg LOCA transient with ASTEC and MELCOR codes

G Agnello[1], S Ederli[2], P Maccari[3], F Mascari[4]

[1] Università degli Studi di Palermo, Dipartimento di Ingegneria, Viale delle Scienze, Edificio 6, 90128, Palermo, Italy
[2] ENEA – Casaccia, Via Anguillarese 301, 00123, Roma, Italy
[3] UNIBO, DIN, Via dei colli 16, 40136, Bologna, Italy
[4] ENEA – Bologna, Via Martiri di Monte Sole 4, 40123, Bologna, Italy

Corresponding author's email: giuseppe.agnello04@unipa.it

Abstract. The analyses of postulated severe accident sequences play a key role for the international nuclear technical scientific community for the study of the effect of possible actions to prevent significant core degradation and mitigate source term release. To simulate the complexity of phenomena involved in a severe accident, computational tools, known as severe accident codes, have been developed in the last decades. In the framework of NUGENIA TA-2 ASCOM project, the analysis of an unmitigated 2-inch cold leg LOCA transient, occurring in a generic western three-loops PWR-900 MWe, has been carried out with the aim to give some insights on the modelling capabilities of these tools and to characterize the differences in the calculations results. The ASTEC V2.2b code (study carried out with ASTEC V2, IRSN all rights reserved, [2021]), and MELCOR 2.2 code have been used in this code-to-code benchmark exercise. In the postulated transient, the unavailability of all active injection coolant systems has been considered and only the injection of accumulators has been assumed as accident mitigation strategy.

1. Introduction

The interest of international nuclear scientific community, after the Chernobyl and, more recently, Fukushima Dai-ichi accident, has focused on the field of Severe Accident (SA) and on the development of new strategies to mitigate core damages and possible releases of Fission Products (FPs) to the environment. To develop and consolidate Severe Accident Management (SAM) measures, the study on SA sequences led to the development of simulation tools, known as SA codes, for simulating the main phenomena occurring in a Nuclear Power Plant (NPP) during postulated accidents. Several experimental programs in the field of SA phenomena have been conducted to validate the models and correlations implemented in the codes and provided a valuable "assessment database" to assess SA simulation tools [1]. However, the analyses of the current state-of-art shows that there is a need to reduce some uncertainties still present [2] and a consequent investigation of phenomena/processes not investigated in detail in geometric prototypical facility with prototypical material should be addressed. In relation to this, for example, the complex multi-physics phenomena taking place during the degradation and relocation of the core material determines uncertainties on the zircaloy area exposed to steam for oxidation process and limited data from full-scale experimental facility are available for code validation. Therefore, discrepancies in some core degradation phenomena can be still observed when comparing

the results as predicted by different simulation tools considering the different core degradation models implemented in the codes [3]. Code-to-code benchmark exercise [4] involving code developers could contribute to identify code modelling differences affecting the codes [5]. Code-to-code exercise involving code users could characterize the user effect on code prediction [3,6]. The present code-to-code benchmark exercise, developed in the framework of NUGENIA TA-2 ASCOM (ASTEC COMmunity) collaborative project [7], coordinated by IRSN, has been conducted to investigate the main discrepancy in predicting thermal-hydraulic and core degradation in-vessel phenomena of ASTEC [8] and MELCOR [9] codes during an unmitigated 2-inch Cold Leg (CL) Loss Of Coolant Accident (LOCA) in a generic PWR 900 MWe three-loops western type.

2. Transient characteristics and hypothesis of the study

The NPP considered in this analysis is a generic PWR-900 MWe three-loops western type and the SA sequence selected for the presented study is an unmitigated Small Break LOCA [4,10] in which only the accumulators are considered available. The accident initiator event considered is a 2-inch break of the CL of loop 1, where the pressurizer (PRZ) is located. The initial plant operation point, before the Start of the Transient (SOT), is the nominal full-power condition. The break event is coupled with the loss of offsite Alternating Current (AC) power and the failure of all the diesel generators determining the unavailability of the following systems: primary pressure control systems (heaters and PRZ spry), Chemical and Volume Control systems (CVCS), Reactor Coolant Pump (RCP) seal injection, Active safety injection systems (High Pressure Injection System, HPIS, and Low Pressure Injection System, LPIS), Motor-driven Auxiliary Feedwater (MDAFW) system. The following hypotheses are also considered: reactor SCRAM and Steam Generators (SGs) isolation at SOT, independent failure of the Turbine Driven Auxiliary Feedwater (TDAFW) pump, no primary boundary structures thermal induced degradation phenomena, primary and secondary side Steam Relief Valves (SRVs) availability throughout the accident evolution, Safety Valves of Pressure Compensator (SEBIM) manually stuck open when the core exit temperature reaches 650°C. The transient has been analyzed until the vessel Lower Head (LH) failure.

3. ASTEC code description and reactor input-deck main characteristics

The ASTEC code (Accident Source Term Evaluation Code) [8], developed by the French "Institut de Radioprotection et de Sûreté Nucléaire" (IRSN), aims at simulating an entire SA sequence in nuclear water-cooled reactors. ASTEC includes several coupled modules that can deal with the different SA phenomena. The code version used in this activity is ASTEC V2.2b. The ASTEC reactor input-deck used is the generic PWR-900 MWe input-deck delivered by IRSN with the ASTEC V2.2b code.

(a)   (b)   (c)
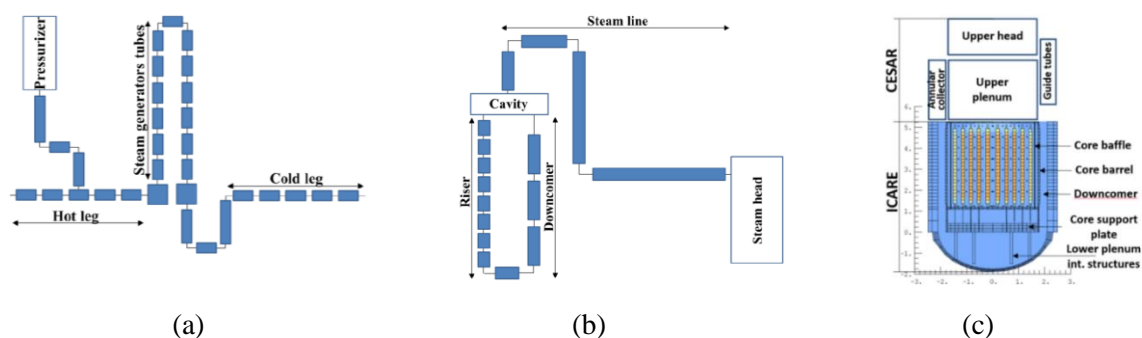
Figure 1. ASTEC Loop 1 (a), SCS (one loop) (b) (CESAR) and RVP (c) (CESAR and ICARE) nodalization [11].

The Primary Cooling System (PCS), part of the Reactor Pressure Vessel (RPV) (Upper Head -UH-, Upper Plenum -UP-, annular collector and the guide tubes) and Secondary Cooling System (SCS) are modelled with the volumes of CESAR module [12], the module of ASTEC dedicated to the simulation of thermal-hydraulic phenomena. The three primary loops are modelled separately: in Figure 1a the loop 1 containing the PRZ is shown. The accumulators have been modelled using special volumes defined as

accumulators, with the availability of multiple dedicated settings (e.g. gas expansion model, etc.). The accumulator opening has been set with a control logic that permits the emergency coolant discharge when the primary pressure falls below the pressure set-point value. The SCS, shown in Figure 1b, includes the SGs and the steam lines. The RPV structures, shown in Figure 1c, from the LH to the upper core plate, are modeled with ICARE module [13], the ASTEC module dedicated to the simulation of the in-vessel core degradation phenomena. The core is divided into 5 radial fluid channels (containing 5 groups of fuel rods) and 16 axial segments and two other fluid channels simulate respectively the core bypass (BP) and the downcomer (DC).

4. MELCOR code description and reactor input-deck main characteristics

MELCOR [9] is a fully integrated SA code, developed at Sandia National Laboratories (SNL) for the US Nuclear Regulatory Commission (USNRC), able to simulate the thermal-hydraulic phenomena in steady-state and transient condition and the main phenomena occurring in a SA. MELCOR can be used with Symbolic Nuclear Analysis Package (SNAP) [14] to develop the nodalization and for the post processing of data. MELCOR has a modular structure and is based on packages simulating a different part of the transient phenomenology. The MELCOR code version used is MELCOR 2.2 18019. The MELCOR nodalization [3,6,10,15,16] of the generic PWR-900 western type three-loops, shown in Figure 2a, developed by using SNAP, was designed to have a reasonable computational time and realistic prediction of the thermal hydraulics and core degradation phenomena.


(a)   (b)
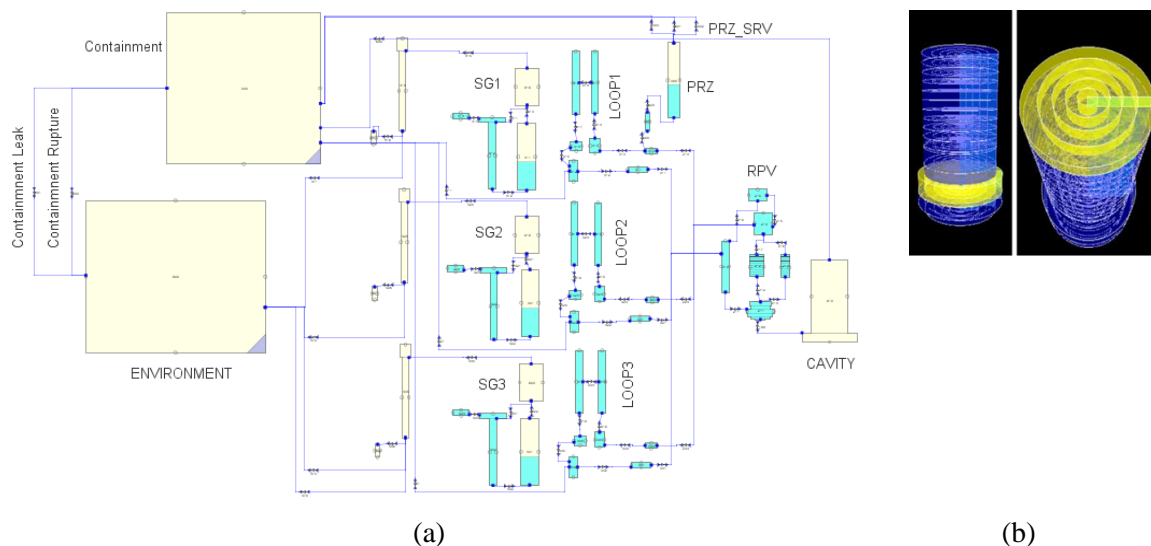
Figure 2. MELCOR PCS, SCS (a) and core (b) nodalization developed using SNAP.

It has been developed considering the plant information's reported in the 2013 Foucher reports [17,18] and the ASTEC input files provided by IRSN during the EU-CESAM project [19]. The prediction capability of this MELCOR input-deck has been already revised along the EU-FASTNET project [20,21] and EU-IVMR project [22,23]. The three loops have been modelled separately. The SG side is composed of three different volumes representing the SG downcomer, the SG riser and the SG cavity. The accumulators have been modelled by one CVH volume for each loop, in adiabatic condition, and by control functions to set the accumulator opening/closing. The accumulators opening begin when the primary pressure falls below the pressure set-point. The thermal-hydraulic CVH nodalization of the RPV features different hydraulic regions simulating Lower Plenum (LP), core, core BP, UP, UH and DC. The core is modelled by a single hydraulic region, CVH package, coupled with the correspondent model of the COR package. A temperature of 2450 K is considered for modelling the melting temperature of the mixture UO_2/ZrO_2. The core, within the COR package, is modelled with 17 axial regions and 6 radial regions; 5 radial regions are used to model the core region, as shown in Figure 2b.

5. Transient evaluation and codes results analysis

5.1. Thermal-hydraulic evolution of the transient

Before the transient simulation, a steady state analysis has been evaluated for both the two codes and the comparison have been already reported in [6]. At the SOT (t = 0 s), as hypothesized in both the codes, reactor SCRAM and the SGs isolation take place. It follows the drop of the core steady fission power to decay power. The break opening determines a primary coolant leakage to the containment with a consequent RPV blowdown and fast PCS pressure decrease. As shown in Figure 3, the primary coolant mass flow rate through the break is greater in ASTEC than in MELCOR in the first 200 s of the transient and, subsequently, it is greater in MELCOR till 1500 s. The total amount of water mass discharged through the break till 1500 s is greater in MELCOR calculation.
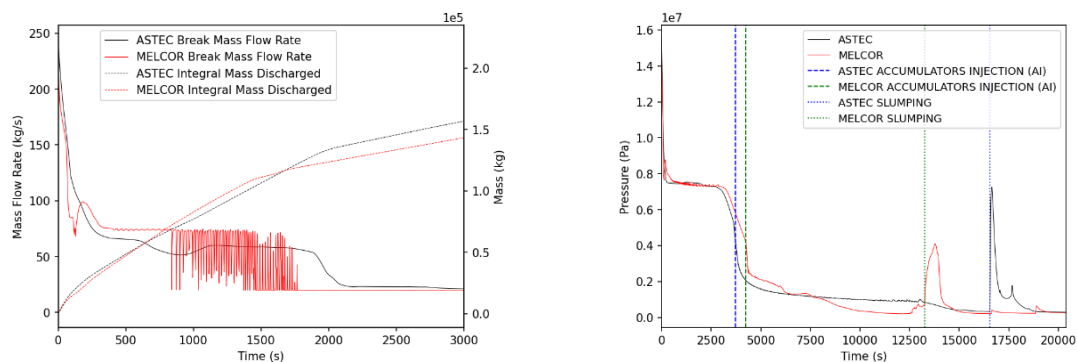
Figure 3. Break mass flow rate and primary coolant mass discharged from the break.

Figure 4. Primary pressure (PRZ pressure).

As shown in Figure 4, along this first blowdown phase, the primary pressure behavior for ASTEC and MELCOR is similar from both a qualitative and quantitative point of view. The isolation of the SGs takes place leading to a SGs secondary side pressure temporary increase: when the pressure set point of SGs SRVs is reached, the SGs start the cycling phase with the release of steam, at about 38 s and 30 s after the SOT in the SG1 respectively in ASTEC and MELCOR. After a rapid depressurization, the primary pressure stabilizes at the saturation pressure. During this phase of the transient, considering the dimension of the break, part of the core decay heat is removed by the coolant discharged through the break and part by the SGs. The primary coolant boil-off determines the decrease of the core collapsed coolant level, as shown in Figure 5 where the relative core collapsed coolant level is reported for the two codes (Bottom of Active Fuel, BAF, is the value 0 and the Top of Active Fuel, TAF, is the value 1). Some discrepancies between the two codes calculations in the core level decrease for the first 2500 s of the transient are underlined: MELCOR simulates a faster decrease of the core collapsed coolant level than ASTEC due to the major quantity of coolant discharged through the break in the first 1500 s of the transient, as shown previously in Figure 3. In term of pressure, after the pressure plateau, this determines a faster pressure decrease in ASTEC than in MELCOR with the consequent start of the accumulator injection at about 3713 s in ASTEC and 4236 s in MELCOR. A different accumulators behavior, in terms of initial water mass, starting time, injection rate and total amount of emergency coolant injected, is also highlighted in Figure 6 where the water mass of accumulator of loop 1 is shown. The accumulators start the injection first in ASTEC than in MELCOR, and the major injection rate of ASTEC, for a longer period, determines a more rapid rise of the core collapsed coolant level than in MELCOR and allows to reach a higher level in the core. The boil-off of the primary fluid continues determining the fluid level decrease which is faster in MELCOR calculation due to the earlier stop of the first accumulators injection at about 6150 s. In ASTEC the accumulators injection continue until about 12900 s with the total accumulators discharge. The core water level reaches the BAF in the ASTEC case at about 3000 s and at about 13000 s after the accumulators injection. In MELCOR

calculation, characterized by an initial slower depressurization, the BAF is reached only after the accumulator injection at about 10000 s.
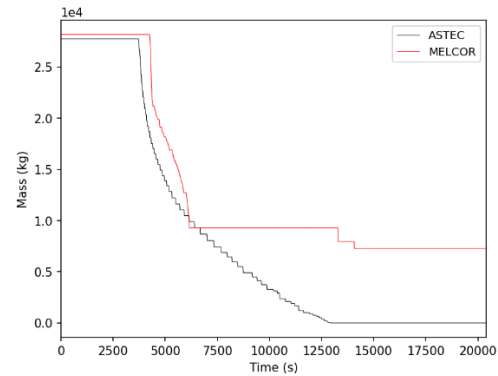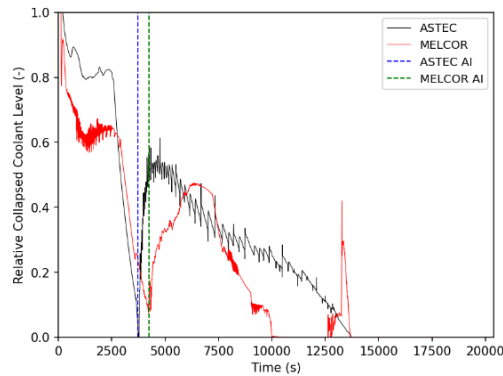
Figure 5. Relative core collapsed coolant level.   **Figure 6.** Loop 1 accumulator water mass.

5.2. Core degradation phase

The core uncovery determines the core heat-up and the onset of chemical reaction between zirconium and steam in the RPV. The energy released by the exothermic oxidation is added to the core decay power causing an acceleration of the heat-up rate with a consequent temperature escalation and hydrogen generation. At about 4000 s, the differences in terms of core uncovery between the two codes determine some discrepancies in terms of cladding temperature, as shown in Figure 7 and Figure 8 where the maximum intact cladding temperature for each fuel ring are represented for ASTEC and MELCOR calculations. When the accumulators start the injection in ASTEC, the maximum cladding temperature presents a value of around 1100 K; in MELCOR, instead, the maximum cladding temperature presents a higher value of around 1600 K; this difference influences the H_2 generation along this phase of the transient. In the MELCOR case the H_2 generation starts and around 100 kg of H_2 are produced before the accumulator injection.
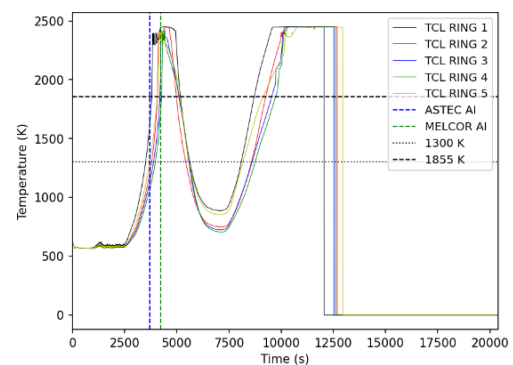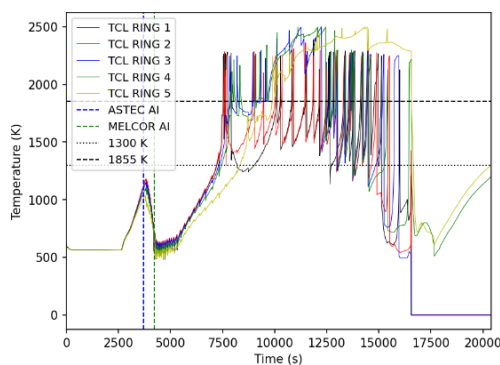

**Figure 7.** ASTEC maximum intact cladding temperature for each fuel ring.   **Figure 8.** MELCOR maximum intact cladding temperature for each fuel ring.

In ASTEC calculation no significant oxidation and consequently a H_2 production, before the accumulator injection, is predicted. ASTEC calculation presents a first cladding temperature peak of about 1250 K at about 3760 s and MELCOR calculation presents a first cladding temperature peak of about 2500 K at about 4300 s. After the partial reflooding of the core, the maximum intact cladding temperature decreases at about 600 K in both the codes predictions. With the cladding temperature decrease, the oxidation rate of Zr and consequently the H_2 and ZrO_2 generation rate stop in MELCOR calculation as shown in Figure 9, 10 and 11 where the H_2 cumulative generation, the Zr, ZrO (only for ASTEC code) and ZrO_2 masses along the transient evolution are reported. At about 5500 s in ASTEC
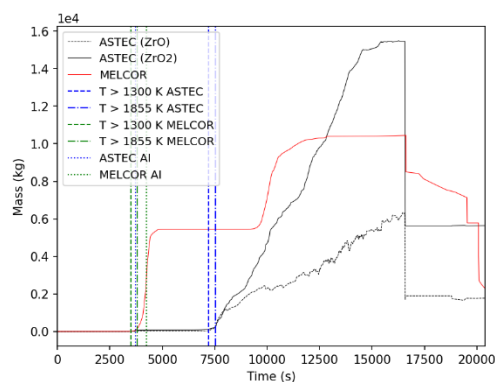
and 7500 s in MELCOR, the core water level returns to decrease and the cladding temperature returns to growing. Then, the H_2 generation starts considerably in ASTEC (at about 7100 s) and starts again in MELCOR (at about 9500 s) after the plateau of about 4200 s.
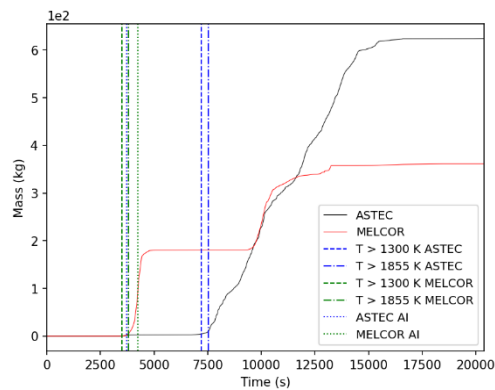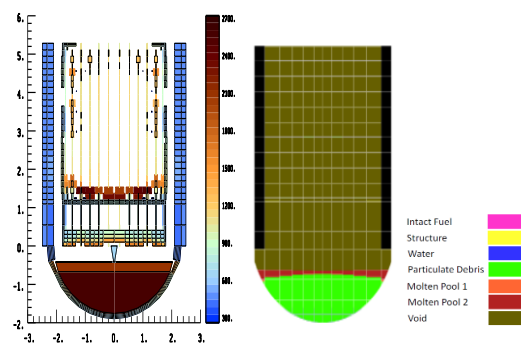

Figure 9. H_2 cumulative generation.
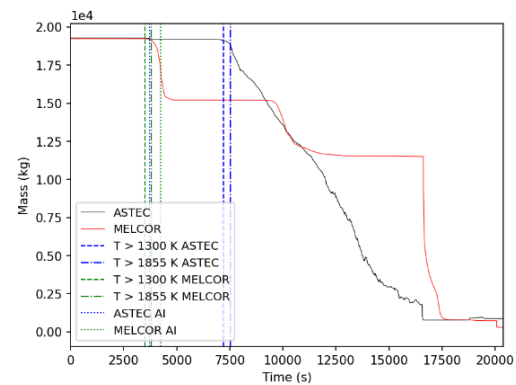
Figure 10. Zr core mass.

Figure 11. ZrO (only for ASTEC case) and ZrO_2 core mass.

Figure 12. ASTEC (left) and MELCOR (right) core composition before lower head failure.

The core collapsed level continues to decrease faster in MELCOR than in ASTEC. Along this phase the core degradation and relocation phenomena progress in both the simulations. The loss of core geometry determines the relocation of core material in the LP (slumping), predicted both in the two codes. The slumping occurs first, at about 13253 s, in MELCOR and later in ASTEC at about 16564 s. The corium relocates to the LP where it remains for a time of about 3830 s in ASTEC and about 6907 s in MELCOR before the LH failure which occurs at about 20160 s in MELCOR and at about 20394 s in ASTEC. These discrepancies could be caused by the difference in the corium behaviour predicted by the two codes. In fact, in ASTEC the corium in the LP is composed of molten corium layers (oxide at the bottom and metal at the top) and the presence of debris bed particles is negligee. In MELCOR the corium in the LP is composed predominantly by particulate debris at the bottom and a small quantity of molten metal at the top, as shown in Figure 12. In Table 1 are presented the relevant phenomenological aspect predicted by ASTEC and MELCOR codes with the specific timings and discrepancies. The total mass of H_2 produced by Zr oxidation process is about 600 kg in ASTEC and 350 kg in MELCOR. One of the reasons of this difference could be the MELCOR prediction of a first generation of H_2 before the accumulator injection; therefore, a first limited degradation of the core takes place. The second accumulator injection determines a further source of steam. Since the H_2 generation depends on the fuel cladding surface available to the reaction with the steam, a less damage core produces more H_2. Furthermore, the accumulators inject more water in ASTEC and more steam is available. Therefore, in ASTEC along the second peak cladding temperature more H_2 is produced.

Table 1. Relevant phenomena aspects predicted by ASTEC and MELCOR codes.

Relevant Phenomenological Aspects [s]	ASTEC	MELCOR	DISCR [%]*
SOT, SCRAM, SGs isolation	0	0	0
SG 1,2,3 cycling inception	38,30,30	30,25,25	21.05,16.67,16.67
Core TAF uncovered	204	126	38.24
H$_2$ generation start	2923	3336	14.13
T > 1300 K (before accumulators injection)	-	3505	-
T > 1855 K (before accumulators injection)	-	3798	-
Start of accumulators 1,2,3 discharge	3713,3713,3713	4236,4238,4238	14.09,14.14,14.14
Core BAF uncover	3773		-
T > 1300 K (after accumulators injection)	7208	8086	12.18
T > 1855 K (after accumulators injection)	7528	8707	15.66
Core BAF uncover	13702	10006	26.97
Slumping	16564	13253	19.99
LH failure	20394	20160	1.15

*discrepancy in the Table 1 has been calculated as the percentage difference between the parameters evaluated by the two codes.

6. Conclusions

In this present work, developed in the framework of NUGENIA TA-2 ASCOM project, a code-to-code benchmark activity with ASTEC and MELCOR codes has been conducted considering a Small Break LOCA initiated by a 2-inch break on the CL of a generic PWR-900 MWe three loops western type. The unavailability of all active injection coolant systems has been considered and the injection of accumulators has been assumed as only accident mitigation strategy. In relation to the phase where thermal-hydraulic phenomena are dominant, the two codes predict the same qualitative behaviour while some quantitative differences are related to break flow rate and the accumulator behaviour: both affect the core level behaviour and the consequent partial or total core uncovery phenomena. This determines the cladding temperature increase and the consequent H$_2$ generation before and after the accumulator injection. Before the accumulator injection a more evident core uncovery, as in the case of MELCOR calculation, can determine a H$_2$ generation and, therefore, limited degraded core. After the accumulator injection, since the H$_2$ generation depends on the fuel cladding surface available to the reaction with the steam, a less damage core can produce more H$_2$, as in the case of ASTEC simulation (350 kg of H$_2$ are produced by MELCOR, 600 kg of H$_2$ are produced by ASTEC). Also, accumulators injection behaviour can have an influence on the H$_2$ generation due to the injection rate and total mass injected. In the case of ASTEC accumulators inject more water and, therefore, more steam is available. Once the accumulators injection ends, the core will start to heat-up again and degradation phenomena start to be dominant. This phase is still characterized by some uncertainties on phenomena such as core melt progression, core relocation to LP, LP debris bed behaviour, and LH failure. Even though MELCOR predicts a faster degradation than ASTEC (also related to the different accumulator behaviour) and a consequent earlier corium relocation to the LP, the different retention time of the corium in the LP leads to limit the code-to-code discrepancy to about 1% for the LH failure event. The observed discrepancies underline some modelling differences between the two codes and details studies are in progress to characterize them as well as the user effect in view of uncertainty estimation. In relation to the user effect, in the case of MELCOR code the effect of the accumulator modelling is under investigation. In fact, in this study a CVH model is used to model the accumulator, but, currently, an accumulator package is available and an adiabatic and isothermal approximations, used for modelling the accumulators gas expansion on the transient progression prediction, are available for the user [4,9].

References

[1] Mascari F, Nakamura H, Ummlnger K, De Rosa F and D'Auria F 2015 *Scaling Issues for the Experimental Characterization of Reactor Coolant System in Integral Test Facilities and Role of System Code as Extrapolation Tool*, Proceedings of NURETH 2015 **6**.

[2] Van Dorsselaere J P, Mustoe J, Power S, Adorni M, Schaffrath A and Nieminen 2016 *Kerntechnik* **81**, Issue 5, pp. 527-534. DOI: https://doi.org/10.3139/124.110734

[3] Mascari F, De La Rosa Blul J C, Sangiorgi M and Bandini G 2019 *Analyses of an Unmitigated*

Station Blackout Transient in a Generic PWR-900 with ASTEC, MAAP and MELCOR Codes, NUREG/IA-0515.

[4]   De la Rosa Blul, Brumm S, Mascari F, Lee S J and Carenini L 2018 *ASTEC-MAAP Comparison of a 2 Inch Cold Leg LOCA until RPV Failure*, Science and Technology of Nuclear Installations, Vol 2018. DOI: https://doi.org/10.1155/2018/9189010

[5]   Belon S, Bouillet C, Topin V, Bonneville H and Andrews N 2017 *Insight of core degradation simulation in integral codes throughout ASTEC/MELCOR crosswalk comparisons and ASTEC sensitivity studies*, Proceedings of the 8th European Review Meeting on Severe Accident Research ERMSAR-2017, Warsaw, Poland, May 16-18, 2017.

[6]   Maccari P, Mascari F, Ederli S and Manservisi A 2021 *J.Phys.: Conf. Ser.* **1868** 012019. DOI: https://doi.org/10.1088/1742-6596/1868/1/012019

[7]   Chatelard P 2018 *ASCOM project overview and description of work*, SARNET-ASCOM-COORDI-P1.

[8]   Chatelard P, Belon S, Bosland L, Carénini L, Coindreau O, Cousin F, Marchetto C, Nowack H, Piar L and Chailan L 2016 *Annals of Nuclear Energy* **93**, pp. 83-93. DOI: https://doi.org/10.1016/j.anucene.2015.12.026

[9]   MELCOR Computer Code Manuals, Vol.1: Primer and Users' Guide, SAND 2015-6691 R; Vol. 2: Reference Manual, SAND 2015-6692 R; Vol. 3: MELCOR Assessment Problems, SAND 2015-6693 R; Sandia National Laboratories, USA.

[10]   Mascari F, Guglielmelli A and De la Rosa Blul J C 2018 *Analysis of a postulated 2-inch Cold Leg LOCA severe accident in a PWR-like 900 MWe with MELCOR code*, Proceedings of the International Conference Nuclear Energy for New Europe, NENE 2018, Portorož, Slovenia, September 10-13.

[11]   Ederli S, Mascari F and Carenini L 2019 *ASTEC simulation of In Vessel Retetion Strategy applied to a generic PWR 900 MWe*, ERMSAR2019, Prague, March 18-20.

[12]   Piar L 2015 *CESAR physical and numerical modelling*, IRSN Report n° PSN-RES/SAG/2015-00332.

[13]   Coindreau O 2016 *ASTEC V2.1: Physical modelling of the ICARE module*.

[14]   Symbolic Nuclear Analysis Package (SNAP) 2021 Users Manual. Applied Programming Technology, Inc. Bloomsburg, PA.

[15]   Mascari F and Ederli S 2019 *Analyses with MELCOR code of an unmitigated SBO scenario with in vessel retention strategy applied to a generic PWR-900 MWe*, 18th International Topical Meeting on Nuclear Reactor Thermal Hydraulics, NURETH 2019, pp. 2497-2510.

[16]   Pescarini M, Mascari F, Mostacci D, De Rosa F, Lombardo C and Giannetti F 2017 *J. Phys.: Conf. Ser.* **923** 012009. DOI: https://doi.org/10.1088/1742-6596/923/1/012009

[17]   Foucher L, ASTEC V20R3 PWR900 Like ASTEC Input Deck, Rapport n° PSNRES/SAG/2013-451.

[18]   Foucher L, ASTEC V20R3, PWR900 Like ASTEC Steady State Calculation, Rapport n° PSN-RES/SAG/2013-466.

[19]   Nowack H, Chatelard P, Chailan L, Hermsmeyer St, Sanchez V and Herranz L 2018 *Annals of Nuclear Energy* **116**, pp. 128-136. DOI: https://doi.org/10.1016/j.anucene.2018.02.021

[20]   https://cordis.europa.eu/project/id/662284/it

[21]   Mascari F et al. 2019 *FASTNET scenarios database development and status*, Proceedings of the 9TH European Review Meeting on Severe Accident Research (ERMSAR2019), Prague, Czech Republic, March 18-20.

[22]   Fichot F, Carénini L, Sangiorgi M, Hermsmeyer S, Miassoedov A, Bechta S, Zdarek J and Guenadou D 2017 *Status of the IVMR Project: First steps Towards a New Methodology to Assess In-Vessel Retention Strategy for High-power Reactors*, Proceedings of the 8th European Review Meeting on Severe Accident Research - ERMSAR-2017 Warsaw, Poland, 16-18 May 2017.

[23]   https://cordis.europa.eu/project/id/662157/it